Journal of Modern Optics
Vol. 53, Nos. 16–17, 10–20 November 2006, 2325–2335

Superfluorescence from dense electron–hole plasmas under high magnetic fields

Y. D. JHO*†§, X. WANG†, J. KONO‡, D. H. REITZE†,
X. WEI§, A. A. BELYANIN¶, V. V. KOCHAROVSKY¶‖,
VL. V. KOCHAROVSKY‖ and G. S. SOLOMON#

†Department of Physics, University of Florida, Gainesville, FL 32611, USA
‡Department of Electrical and Computer Engineering,
Rice University, Houston, TX 77005, USA
§National High Magnetic Field Laboratory, Florida State University,
Tallahassee, FL 32310, USA
¶Department of Physics, Texas AM University,
College Station, Texas 77843, USA
‖Russian Academy of Sciences, Institute of Applied Physics,
603950 Nizhny Novgorod, Russia
#Solid-State Laboratories, Stanford University,
Stanford, CA 94305, USA

(*Received 15 February 2006; in final form 8 May 2006*)

Ultrafast optical excitation of a dense electron–hole plasma in $In_xGa_{1-x}As$ multiple quantum wells in high magnetic fields (>20T) produces cooperative radiative recombination between conduction and valence band Landau levels (LL). Above a critical threshold, the emission is characterized by very narrow LL line widths, superlinear increase with increasing field and laser excitation fluence, and stochastic directionality from shot to shot. Here, we investigate the effects of temperature and excitation geometry on the emission properties.

1. Introduction

The application of strong laser fields to explore quantum optical phenomena has played a major role in our understanding of the interaction of light with atomic systems. In particular, superfluorescence (SF) is one of most exotic cooperative phenomena known in quantum optics [1–3]. In SF, an incoherently prepared system of N inverted atoms develops macroscopic coherence self-consistently through a subtle quantum process starting from vacuum fluctuations. The resultant macroscopic dipole decays superradiantly [4, 5] producing a burst of coherent radiation.

*Corresponding author. Email: ■■■

Journal of Modern Optics
ISSN 0950–0340 print/ISSN 1362–3044 online
http://www.tandf.co.uk/journals
DOI: 10.1080/09500340600893867

Superfluorescence has been observed in atomic gases [6, 7] and rarefied impurities in crystals [8–10].

SF is characterized by several distinguishing physical signatures and time scales. A pure or ideal SF pulse [1] is bright (intensity $\propto N^2$), short (duration $\propto 1/N$ is shorter than the dephasing time), and highly directional. In addition, a SF pulse is produced after a certain delay time during which mutual coherence between individual optical dipoles is established. The fluctuations of the optical polarization of a sample grow from initially incoherent quantum noise and reach a macroscopic level. Because of this fluctuating nature, SF is intrinsically random; both the delay time and the direction of the emitted burst will vary from shot to shot. SF requires that macroscopic coherence be established on time scales shorter than homogeneous dephasing time T_2. Also, note that SF is different from superradiance: the latter develops in a system in which the coherent macroscopic polarization has been initially excited by an external laser field. An example of superradiance is the accelerated radiative decay of excitons created by a resonant coherent laser pulse [11].

For the case of semiconductor systems, extensive investigations on quantum optical analogues in condensed matter and mesoscopic systems have followed [12]. However, a variety of well-known strong field quantum optical phenomena remain for the most part unexplored because they require tunable ultrafast lasers to create solid state 'atoms' (excitons) and probe them on time scales faster than decoherence times (typically ps or less) [13], in combination with high magnetic fields to freeze the motion of 'atoms' and controllably tune their energy levels. Heretofore, the scarcity of tunable ultrafast spectroscopic capabilities at high magnetic field facilities has limited progress in this area. To enable these investigations, we have developed an ultrafast spectroscopy laboratory at the DC High Field Facility of the National High Magnetic Field Laboratory, with the capability of probing over the 200 nm–20 μm wavelength range with 150 fs temporal resolution in fields up to 31T.

Electron–hole (e–h) plasmas exhibit strong carrier–carrier correlations at low temperatures in high magnetic fields. For example, band gap renormalization (BGR) [14], carrier effective mass renormalization [15, 16] and spin-splitting effects [17] have been investigated in $In_xGa_{1-x}As$ and GaAs quantum wells (QWs) using continuous wave (CW) and nanosecond pulse excitations at relatively low laser intensities. We have investigated an undoped $In_xGa_{1-x}As$ QW system placed in a strong perpendicular magnetic field. The strong magnetic field fully quantizes the (already 2D) QW system into an atomic-like system with a series of Landau levels (LLs) and thus strongly enhances the densities of states. The degeneracy of each LL increases linearly with the magnetic field (as eB/h), which significantly increases N. When combined with an intense femtosecond laser pulse, it is possible to create an extremely dense ($>10^{13}\,cm^2$) e–h plasma.

Recently, we have observed strong, highly directional emission from dense e–h plasmas in $In_xGa_{1-x}As$ in high magnetic fields excited by intense femtosecond pulses [18]. A strong correlation between the magnetic field strength (pump laser fluence) and the linewidth and power scaling of emission strength was observed. In an intermediate excitation regime, the emission indicated amplified spontaneous emission, while above a critical threshold, the scaling of the emission linewidth and

power were seen, consistent with predictions for superflourescence (SF) in quantum wells [19]. In addition, strong evidence for the cooperative nature of the emission process at high excitation fluence was found in the stochastic nature of the emission direction; strong and randomly varying shot-to-shot fluctuations of the in-plane emission direction were observed.

In this paper, we investigate how the collective emission process is influenced by resonant transition energies, temperature and the excitation focal geometry. We find that the formation of high gain emission (SF or ASE) can be suppressed by resonant absorption features, In addition, the temperature scaling of the critical threshold for the formation of SF can be explained by a simple model based on phonon occupation. Finally, we demonstrate that the direction of emission can be efficiently controlled by tailoring the shape of the excitation geometry.

2. Experimental methods

Experiments were performed on two $In_{0.2}Ga_{0.8}As/GaAs$ quantum well samples, consisting of 15 layers of 8 nm thick QWs separated by 15 nm GaAs barriers, grown by molecular beam epitaxy at 430°C (S1) and 390°C (S2). We used a 775 nm Ti:sapphire regenerative amplifier to excite the sample. Pulse widths of 150 fs were used and the pump fluence was fixed at $\sim 0.62\,\mathrm{mJ\,cm^{-2}}$. A total carrier density of 10^{12} e–h pairs $\mathrm{cm^{-2}}$ was generated for pump fluence of $0.01\,\mathrm{mJ\,cm^{-2}}$. As shown in figure 1(*a*), the excitation beam was delivered through free space into a Bitter-type magnet, and the plane of the QW was perpendicular to B with field up to 30T. Emitted photoluminescence (PL) was collected using optical fibres from the opposite face (centre fibre) and cleaved edges of the sample by using a right-angle micro-prism (edge fibre) and analysed with a grating spectrometer equipped with a

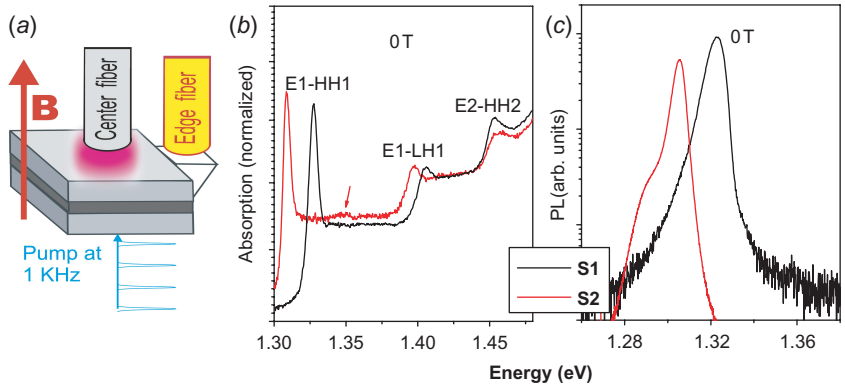

Figure 1. (*a*) Experimental schematic showing free space excitation and collection via fibres. (*b*) Absorption spectra at zero field for samples S1 (black) and S2 (red) at low densities. The arrow shows an optically forbidden state E1-HH2. (*c*) Low carrier-density photoluminescence spectra at zero field for samples S1 (black) and S2 (red). (The colour version of this figure is included in the online version of the journal.)

charge-coupled device detector. Each spectrum consisted of the emission from approximately 1000 pulses. The temperature was fixed at 10 K unless stated otherwise. The sample area and the spot diameter were $3 \times 3\,\mathrm{mm}^2$ and 0.5 mm, respectively. The collection area of the prisms was $1 \times 1\,\mathrm{mm}^2$, and the computed acceptance angle based on geometric considerations was $\sim 40^\circ$. Excitation at 775 nm creates the initial e–h plasma high in the bands with an excess energy of 150 meV above the GaAs barrier band gap. The energy difference between the initial carrier states and the 0–0 LL in QWs† is therefore more than 270 meV. The initially excited carriers scatter with a very short relaxation time (~a few fs) and then thermalize and relax into the well LLs, becoming quantized with a longer effective T_2. The resulting e–h plasma in the individual LLs is thus initially *completely incoherent*.

To characterize the optical properties of our samples, in figure 1(*b*) and (*c*), we display the zero field absorption and PL spectra of S1 and S2 excited by a white-light from a tungsten lamp and a He : Ne laser respectively. The three prominent peaks in figure 1(*b*), indicated by E1-HH1, E1-LH1 and E2-HH2, are lowest heavy-hole (HH) exciton, lowest light-hole (LH) exciton and second lowest HH exciton state, respectively. The arrow at a broad feature around 1.35 eV in S2 is the E1-HH2 transition which is optically forbidden without very strong strain. Sample S1 (grown at the higher temperature) exhibits an HH–LH splitting of 78 meV while S2 has a HH–LH splitting of 89 meV. In general, the amount of uniaxial strain present in a system increases the HH–LH splitting (although there is no quantitative model for the strain variations via different sample growth temperatures) [21]. Even though the HH–LH splitting energies are of similar magnitude in S1 and S2, the lowered resonance energy in S2 together with the much reduced PL emission as shown in figure 1(*c*) turns out to be critical for SF generation as we show below.

3. Results and discussion

We first discuss the physical basis for cooperative emission in semiconductor quantum wells. The key parameter that determines the growth rate of cooperative spontaneous decay is the strength of the coupling between the electromagnetic field and optical polarization, expressible via the so-called cooperative frequency ω_c [2, 19]. Specifically, in order to observe SF from a system of e–h pairs in a semiconductor quantum well, ω_c must be greater than $2/T_2$ (or $2/(T_2T_2^*)^{1/2}$ for a system with inhomogeneous broadening time $T_2^* < T_2$). SF develops with the growth rate $g \approx \omega_c^2 T_E/4 \propto N$ when ω_c is smaller than the field dissipation rate: $1/(T_2T_2^*)^{1/2} < \omega_c/2 < 1/T_E$. When the cooperative frequency becomes greater than the field dissipation rate, $\omega_c/2 > 1/T_E, 1/T_2$, the growth rate reaches its maximum value $g \approx \omega_c/2 \propto N^{1/2}$ and the intensity of a SF pulse scales as $I_{SF} \equiv \hbar\omega N/\tau_{SF} \propto N^{3/2} \propto B^{3/2}$, with the SF pulse duration $\tau_{SF} \approx 2/g \leq T_2$.

†The high-field Landau notation is used to specify a QW electron–hole plasma in a magnetic field; for low-field–high-field correspondence, see, e.g. [20].

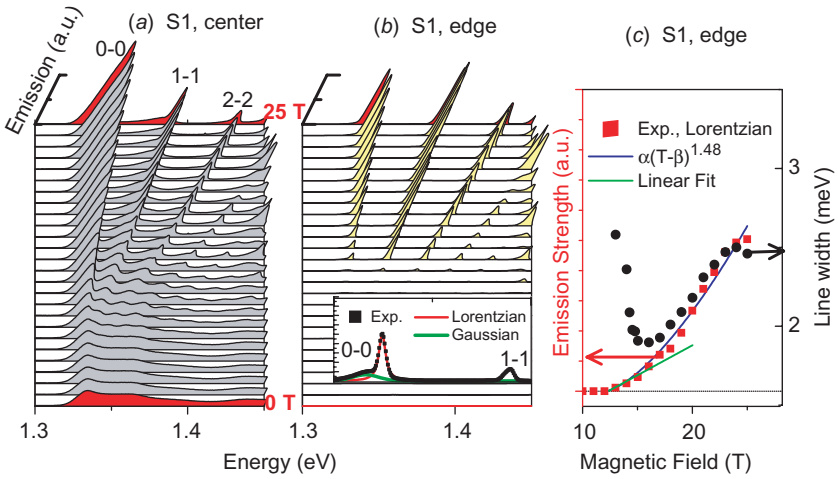

Figure 2. Emission spectra for sample S1 as a function of magnetic field (*a*) for emission through sample above the excitation spot along the laser propagation direction and (*b*) for in-plane emission in an edge collection geometry. (*c*) Emission strength and linewidth of the narrow Lorentzian shaped peak from the 0–0 LL versus magnetic field. The inset of (*b*) shows the fitting method for determining the relative contributions of the 0–0 LL emission using a Lorentzian for the sharp peak and a Gaussian for the broader lower-energy side peak. (The colour version of this figure is included in the online version of the journal.)

Here T_E is the photon lifetime for a given field mode determined by the geometry of a sample. Before reaching the densities for SF formation to occur, the incoherent process of amplified spontaneous emission (ASE) exists in the regime of low inversion density and long photon lifetime with its intensity $I_{\mathrm{ASE}} \propto N \propto B$.

The conditions for achieved SF emission, when evaluated for semiconductors, turns out to be experimentally challenging due to the short dephasing times, and thus it places stringent limits on the types of systems that can be investigated. However, cooperative recombination is predicted to be achievable in systems with reduced dimensionality due to the enhancement of density of states [19]. In our structure, the minimum carrier density for generating SF is estimated at $5 \times 10^{12}\,\mathrm{cm}^{-3}$.

Figure 2 displays emission spectra as a function of magnetic field for case 2(*a*) when collecting light from the opposite side of the sample above the pump spot (denoted by 'centre') and 2(*b*) when collecting at the sample edge perpendicular to the excitation direction ('edge') in sample S1. The spectra in figure 2(*a*) and 2(*b*) both show well-defined higher LL states reported in previous studies [15, 16]. However, in figure 2(*a*), we observe, with increasing *B*, narrow features appear above 13T from the high-energy side, and become dominant at higher *B*. More interestingly in the case of edge emission (figure 2(*b*)), the sharp features emerge from the high-energy side of the broad feature at much higher efficiency: e.g. the integrated emission strength of the sharp feature in the 0-0 LL at 25T was 70 times stronger than the broad spontaneous emission at 8T.

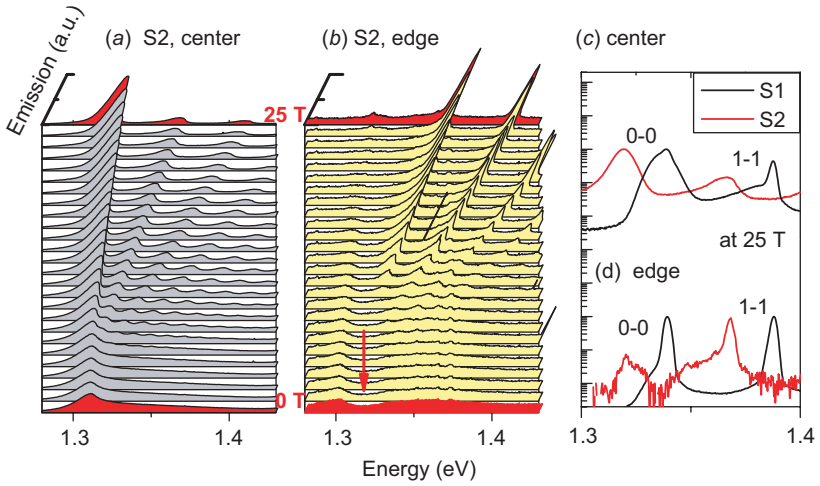

Figure 3. Emission spectra from sample S2 as a function of magnetic field, (*a*) for emission through sample above the excitation spot along the laser propagation direction and (*b*) for in-plane emission in an edge collection geometry. Comparative emission spectra at 25 T from sample S1 (black) and S2 (red) obtained from (*c*) centre collection geometry and (*b*) edge collection geometry. (The colour version of this figure is included in the online version of the journal.)

To analyse the scaling of the signal with B, the integrated strength of the 0–0 LL emission was well fitted by summing a Lorentzian lineshape for the narrow high energy blueshifted feature and a Gaussian lineshape for the broad low energy redshifted feature, as sketched in the inset figure of figure 2(*b*). The Gaussian lineshape is typical for spontaneous emission (SE) while the Lorentzian lineshape originates from homogeneously broadened systems. From the lineshape analysis, we obtained the emission intensity trace of the Lorentzian feature (red squares) in figure 2(*c*). Below 12T, narrow emission is not observed. In the range 12–14T, the signal grows linearly (green lines) with B. Above 14T, the emission strength becomes superlinear (blue lines) with the integrated signal $S \propto B^{3/2}$. The linewidths (black circles), also plotted in figure 3(*c*) reveal a correlation with the emission strength. In the linear regime, the linewidth *decreases* monotonically both versus B until the emission becomes superlinear, where the linewidth begins to *increase*. When the laser spot was increased (decreased) to 3 mm (0.1 mm), narrow emission was observed, but both the integrated signal S and the linewidth exhibited qualitatively different scaling, and in both of these cases, the linewidth monotonically decreased with increasing fluence [18]. Superlinear scaling was observed only when the pump spot-size is 0.5 mm, approximately equal to the theoretically predicted coherence length for SF emission in QWs, $L_c \sim c\tau_{SF} \ln (I_{SF}/I_{SE})$.

In order to examine how the emissions depend on the background optical properties of a sample, we measured the PL spectra in S2 under the same conditions as in figure 2. Figure 3(*a*) shows the emission spectra measured for centre collection

geometry as a function of B. Despite the clear emission features from high LLs, the sharp features from the high energy side of the LLs are absent in figure 3(*a*). Significantly, in the edge collection geometry data of figure 3(*b*), the spontaneous broad feature from 0-0 LL is suppressed up to a very high field range, and the spectra evidence a broad absorption dip centred at 1.32 eV (emphasized by an arrow in figure 3(*b*)). The narrow line emissions from the higher LL states become stronger as their spectral positions shift in energy *above* the absorption dip. Nonetheless, the broad absorption feature at 1.32 eV prevents the formation of a sharp emission feature. We interpret this as arising from the loss due to absorption which competes with the gain g near 1.32 eV, effectively suppressing ASE or SF emission in that spectral region. Figure 3(*c*) compares the emissions from S2 (red lines) to those from S1 (black lines). For comparative purposes, the spectra were normalized to have the same maximum in figure 3(*c*) and (*d*). It is clear that the Lorentzian-shaped sharp features are only observed in S1 in figure 3(*c*). On the other hand, in the edge emission results of figure 3(*d*), the sharp feature in 0–0 LL of S2 is red-shifted in clear contrast to 1–1 LL, which shows a blue-shifted feature.

The blue shift (for all S1 stimulated emission features) or red shift (for the S2 0–0 LL emission) comes about due to competition between gain and absorption loss over light propagation. An additional requirement for achieving SF [18] is the presence of gain guiding. A detailed model of in-plane light propagation in our structures indicates that the radiation is guided by the multiple QW layer in the pumped region due to polariton dispersion. Once the radiation leaves that region, it diverges such that very little gets coupled back to the guided mode, suppressing feedback. The blue-shifted emission in figure 3(*c*) S1 and on the 1-1 LL transition in S2 in the edge collection geometry arises from a refractive index enhancement on the *high energy* side of the inverted interband LL transition in the pumped region, leading to an increase in the overlap factor of the radiation with the active multiple QW region by 10^3 in the pumped region. Self-guiding in the pumped region is essential in this system for achieving high gain ASE or SF. In S2, the blue shift arising from the self-guiding is reduced or totally absent for the 0–0 LL radiation due to the enhanced absorption loss at 1.32 eV and concomitant lower quantum efficiency (cf. figure 1(*c*)).

We now turn to a discussion of the temperature and critical magnetic field dependence of threshold SF emission. In figure 4(*a*), we display the emission spectra in S1 at 110 K as a function of B up to 30T. We observe sharp features from the 0–0 at a much higher magnetic field at $\sim$23T. In addition, the sharp features tend to appear from higher LLs at lower fields with respect to the 0–0 LL as the field is increased. As we follow the threshold field $B_c(T)$ for 0–0 LL (red squares) and for 1-1 LL (black squares) sharp feature in figure 4(*b*), we observe it is more rapidly increasing above 50 K. Here, we define B_c as the critical field for the appearance of narrow linewidth emission. Even though the B_{SF} is not coincident with B_c since the sharp emission feature is generated by both the ASE and SF, we will presume their temperature variation is similar. First, note that the critical magnetic field B_{SF} for SF generation is obtained from a relation between ω_c ($\propto N^{1/2}$) and the dephasing rate $2/T_2$ [18, 19], $\omega_c > 2/T_2$. The LLs density of states is given by $N = eB/h$,

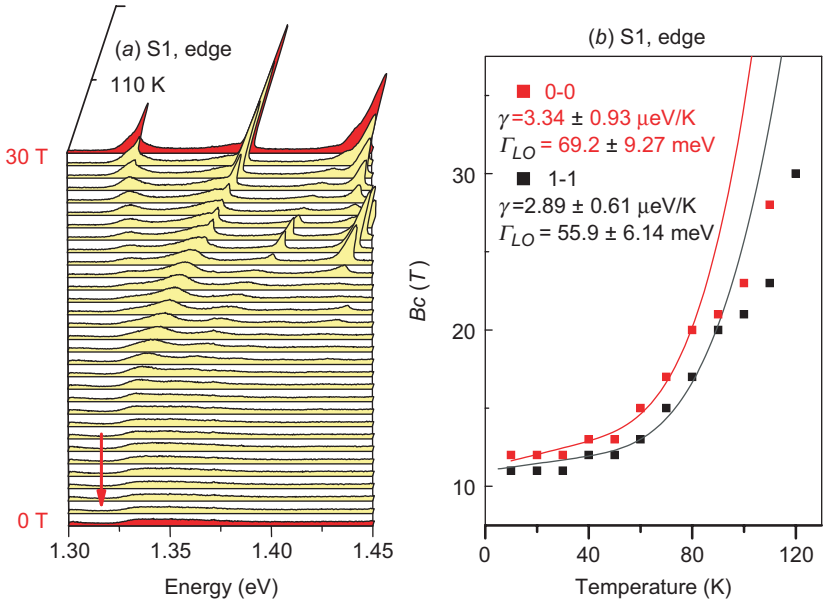

Figure 4. (*a*) Emission spectra from sample S1 at $T = 110\,\mathrm{K}$. (*b*) The threshold field $B_c(T)$ for the 0-0 LL (red scattered line) and for the 1-1 LL (black scattered line) sharp emission features as a function of temperature. The solid lines are fittings based on acoustic and optical phonon contributions from equation (2). (The colour version of this figure is included in the online version of the journal.)

i.e. proportional to B and therefore to ω_c^2. For electron–phonon scattering, the dephasing rate $2/T_2$ can be expressed phenomenologically as

$$2/T_2 \propto \Gamma_0 + \gamma T + \Gamma_{\mathrm{LO}}/[\exp(E_{\mathrm{LO}}/k_{\mathrm{B}}T) - 1], \tag{1}$$

where Γ_0 is the width due to the inhomogeneous broadening and γ (Γ_{LO}) is the fitting parameter which measures the interaction with acoustic phonon (polar LO phonons). Thus, writing $eB_{\mathrm{SF}}/h \propto \omega_c^2 = (2/T_2)^2$, we find

$$B_{\mathrm{SF}} \propto (\Gamma_0 + \gamma T + \Gamma_{\mathrm{LO}}/[\exp(E_{\mathrm{LO}}/k_{\mathrm{B}}T) - 1])^2, \tag{2}$$

since the LO phonon energy E_{LO} in our sample structure, which is expected to be similar to that of GaAs-based QW (~36 meV), is much larger than thermal energy ($k_{\mathrm{B}}T$) in our temperature range, we tentatively identify the acoustic phonon contribution as a dominant temperature mechanism for varying B_{SF}. The red (black) curve in figure 4(*b*) is the fitting based on equation (2) for 0–0 LL (1–1 LL), where we can obtain the comparative values of γ/Γ_0 and $\Gamma_{\mathrm{LO}}/\Gamma_0$, respectively. When Γ_0 being assumed to be the same with the minimum linewidth obtained from figure 2(*c*) (=1.9 meV), γ (Γ_{LO}) is smaller (larger) than that for the 2-dimensional exciton case by 2–3 times (3–4 times) [22] while being very similar to the zero-dimensional case [23]. The deviation of the fitting curve above 80 K for 0–0 LL and above 90 K for 1–1 LL is possibly associated with carrier

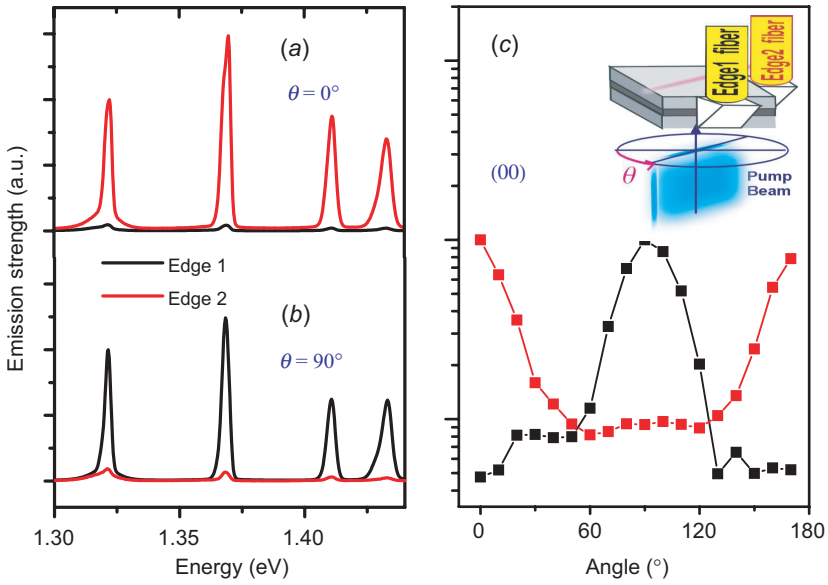

Figure 5. Edge emission spectra measured from two orthogonally aligned fibres for the angle θ at (*a*) 0° and (*b*) 90°, where θ is the angular separation between the longer beam axis and the direction of edge 2 fibre as shown in the inset figure of (*c*). In (*c*), the emission strength of 0-0 LL is plotted for edge 1 (black) and edge 2 (red) as a function of angle. (The colour version of this figure is included in the online version of the journal.)

delocalization and/or deionized impurities at high temperatures [24]. Γ_0 (~1.9 meV) indicates the SF pulse duration is shorter than 330 fs ($=2\hbar/\Gamma_0$) while the temperature dependence of $B_c(T)$ agrees with the dephasing dynamics in a zero-dimensional system.

Finally, we show that it is possible to control the SF emission orientation through tailoring the geometry of the gain region. Using a cylindrical lens to generate a rod-like 3 mm × 0.5 mm excitation region, figure 5 shows the emitted output as a function of angle θ from 0° to 180° (see inset of figure 5(*c*)) for a pump fluence of 0.02 mJ cm^{-2} and 25T magnetic field. The output intensity follows the orientation of the long axis of the gain region, with the relative emission strength from two edges reversed as the angle is rotated by 90°. Tracing the output intensity displayed in figure 5 for edges 1 (black) and 2 (red), the emission is highly directional with a full-width-at-half-maximum of 40°. This value is comparable to the acceptance angle of our measurement, indicating that for this excitation geometry the emission is highly directional. The variance in emitted power by 20 times between two directions is quite reasonable, since the gain should scale exponentially with propagation length, $\exp(1.5/0.5) \sim 20$. Thus, the SF emission direction can be manipulated through tailoring of the gain geometry. However, this is not the unique feature of SF. The same behaviour is expected from high-gain ASE.

4. Conclusion

We have performed magneto-photoluminescence measurements in In_xGa_{1-x} As multiple quantum wells in high magnetic fields using intense femtosecond pulses. The resulting density and energy confinement is sufficient to generate a spontaneous macroscopic polarization that decays through the emission of SF pulses. Our experiments probe the appropriate conditions for observing SF by exploiting its spectral features and dependence on the resonance energies, temperature and focal geometry.

Acknowledgments

This work was supported by the NSF ITR program (DMR-032547) and the NHMFL In-house Science Program. A portion of this work was performed at the National High Magnetic Field Laboratory, supported by NSF Cooperative Agreement No. DMR-0084173 and by the State of Florida. A.B. acknowledges the support from the NSF CAREER program (0547019) and NSF PIRE and ERC programs.

References

[1] See, e.g. A.E. Siegman, *Lasers* (University Science Books, Sausalito, 1986), p. 549.
[2] V.V. Zheleznyakov, V.V. Kocharovsky and Vl.V. Kocharovsky, Sov. Phys. Usp. **32** 835 (1989).
[3] R. Bonifacio and L.A. Luiato, Phys. Rev. A **11** 1507 (1975).
[4] R.H. Dicke, Phys. Rev. **93** 99 (1954).
[5] N.E. Rehler and J.H. Eberly, Phys. Rev. A **3** 1735 (1971).
[6] N. Skribanowitz, *et al*., Phys. Rev. Lett. **30** 309 (1973).
[7] H.M. Gibbs, *et al*., Phys. Rev. Lett. **39** 547 (1977).
[8] R. Florian, *et al*., Solid State Commun. **42** 55 (1982).
[9] P.V. Zinoviev, *et al*., Sov. Phys. JETP **58** 1129 (1983).
[10] M.S. Malcuit, *et al*., Phys. Rev. Lett. **59** 1189 (1987).
[11] T. Tokihiro, Y. Manabe and E. Hanamura, Phys. Rev. B **51** 007655 (1995)
[12] Y. Yamamoto and A. Imamoglu, *Mesoscopic Quantum Optics* (John Wiley & Sons, New York, 1999).
[13] See, e.g. J. Shah, *Ultrafast Spectroscopy of Semiconductors and Semiconductor Nanostructures* (Springer-Verlag, Berlin, 1999).
[14] G. Tränkle, *et al*., Phys. Rev. Lett. **58** 419 (1987).
[15] L.V. Butov, *et al*., Phys. Rev. **B44** 10680 (1991).
[16] M. Potemski, *et al*., Solid State Commun. **75** 185 (1990).
[17] L.V. Butov, *et al*., Phys. Rev. B **48** 17933 (1993).
[18] Y.D. Jho, X. Wang, J. Kono, *et al*., Phys. Rev. Lett. (2006) accepted [arXiv:cond-matt/0601483].
[19] A.A. Belyanin, *et al*., Quantum Semiclass. Opt. **9** 1 (1997); A.A. Belyanin, *et al*., Quantum Semiclass. Opt. **10** L13 (1998); A.A. Belyanin, *et al*., Laser Phys. **13** 161 (2003).

[20] A.H. MacDonald and D.S. Ritchie, Phys. Rev. B **33** 8336 (1986).
[21] Y.D. Jho, F.V. Kyrychenko, J. Kono, *et al*., Phys. Rev. B **72** 045340 (2005).
[22] H. Zhao, *et al*., Phys. Rev. B **66** 085337 (2002).
[23] I. Favero, *et al*., Phys. Rev. B **68** 233301 (2003).
[24] J. Lee, E.S. Koteles and M.O. Vassell, Phys. Rev. B **33** 5512 (1986).